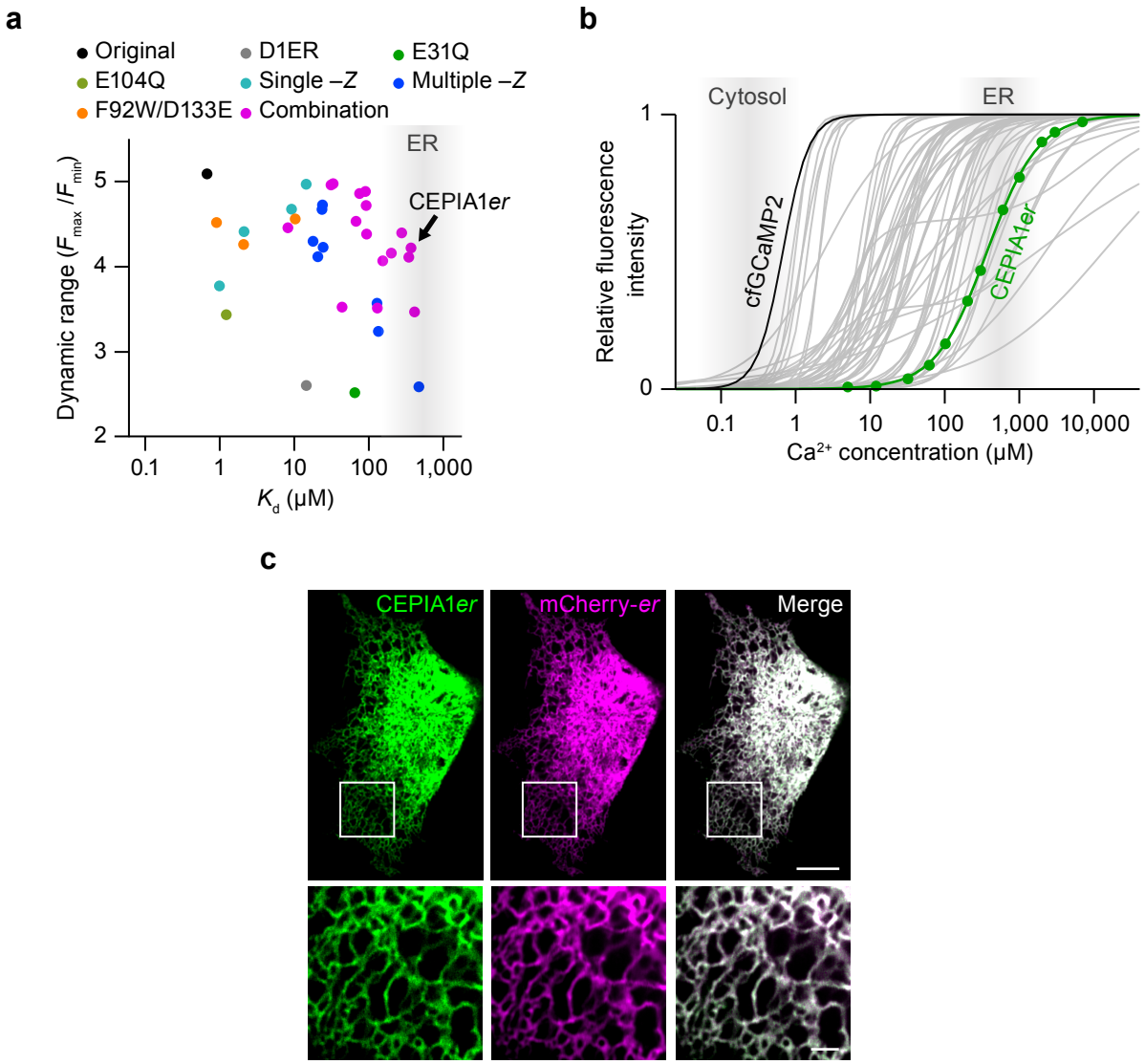

Supplementary Figure 1. Construction of CEPIA1*er*.

(**a**) Scatter chart of cfGCaMP2 variants with respect to Ca^{2+} affinity (K_d) and dynamic range (F_{max}/F_{min}). Introduced amino acid substitutions are categorized by color: original cfGCaMP2 (black), substitutions of previously reported ER Ca^{2+} indicators (gray, green and light green), a substitution at single *–Z* position (cyan), substitutions in multiple *–Z* positions (blue), substitutions at F92W and/or D133E (orange), combinational substitutions at *–Z* positions and F92W/D133E (magenta). Data point for CEPIA1*er* is indicated by an arrow. Putative range of Ca^{2+} concentration in the ER is indicated (gray box).

(**b**) *In vitro* Ca^{2+} titration curves of the recombinant proteins of the original cfGCaMP2 (black) and its variants (gray or green, $n = 58$). For clarity, only the fitted Hill plot curves are shown except for CEPIA1*er*, for which data points are also shown. Putative ranges of Ca^{2+} concentration in the cytosol and ER are indicated (gray boxes).

(**c**) Subcellular distribution of CEPIA1*er* and ER-targeted mCherry (with calreticulin signal sequence) in a HeLa cell. Note that the ER-signal sequence in CEPIA1*er* is different from that of mCherry-er. The images within the white boxes were expanded. Scale bars, 10 μm (upper) and 2 μm (lower).

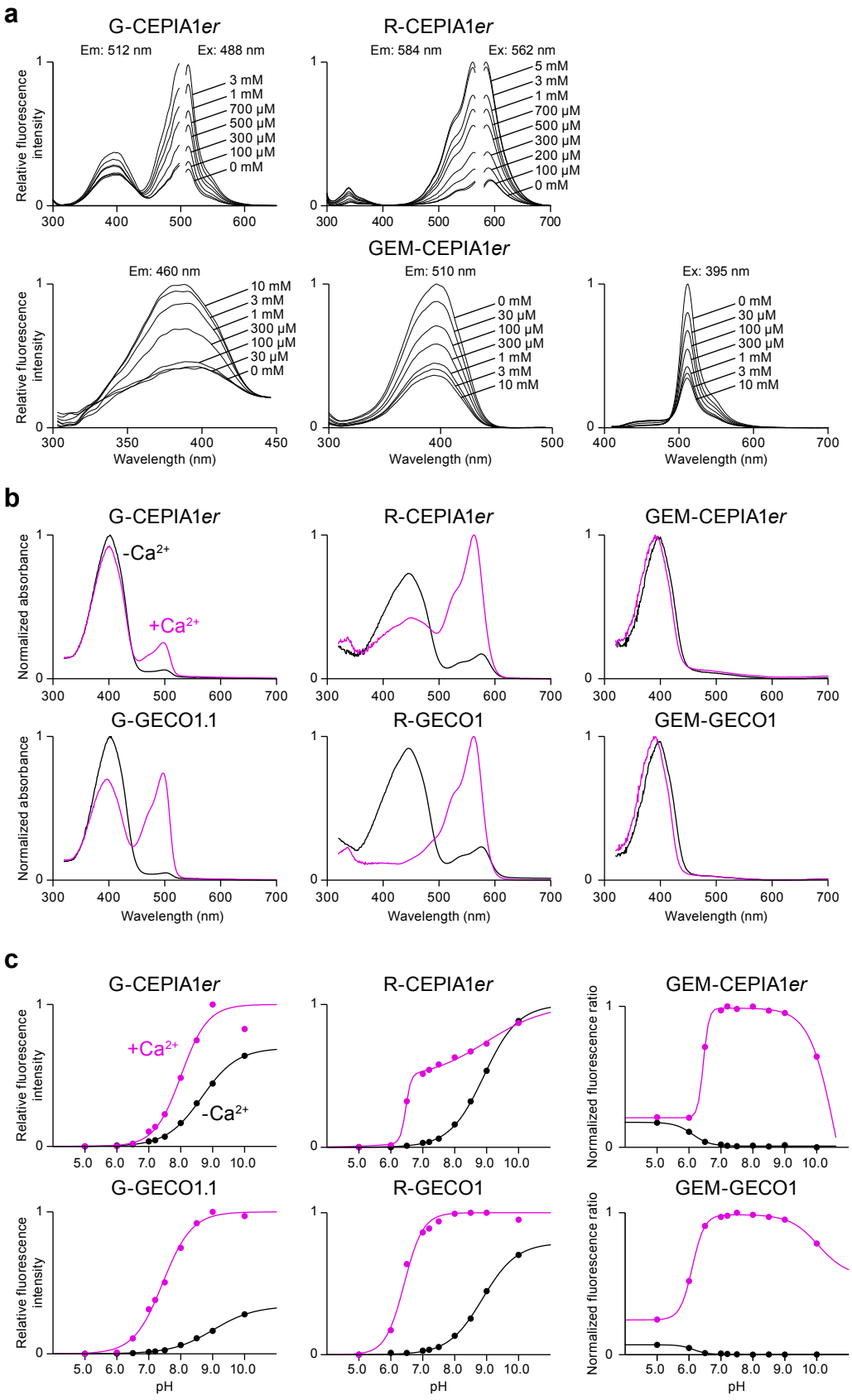
a
G-CEPIA1er
Em: 512 nm
Ex: 488 nm
3 mM
1 mM
700 µM
500 µM
300 µM
100 µM
0 mM
R-CEPIA1er
Em: 584 nm
Ex: 562 nm
5 mM
3 mM
1 mM
700 µM
500 µM
300 µM
200 µM
100 µM
0 mM
GEM-CEPIA1er
Em: 460 nm
10 mM
3 mM
1 mM
300 µM
100 µM
30 µM
0 mM
Em: 510 nm
0 mM
30 µM
100 µM
300 µM
1 mM
3 mM
10 mM
Ex: 395 nm
0 mM
30 µM
100 µM
300 µM
1 mM
3 mM
10 mM
Relative fluorescence intensity
Wavelength (nm)
b
G-CEPIA1er
R-CEPIA1er
GEM-CEPIA1er
-Ca2+
+Ca2+
G-GECO1.1
R-GECO1
GEM-GECO1
Normalized absorbance
Wavelength (nm)
c
G-CEPIA1er
R-CEPIA1er
GEM-CEPIA1er
+Ca2+
-Ca2+
G-GECO1.1
R-GECO1
GEM-GECO1
Relative fluorescence intensity
Normalized fluorescence ratio
pH

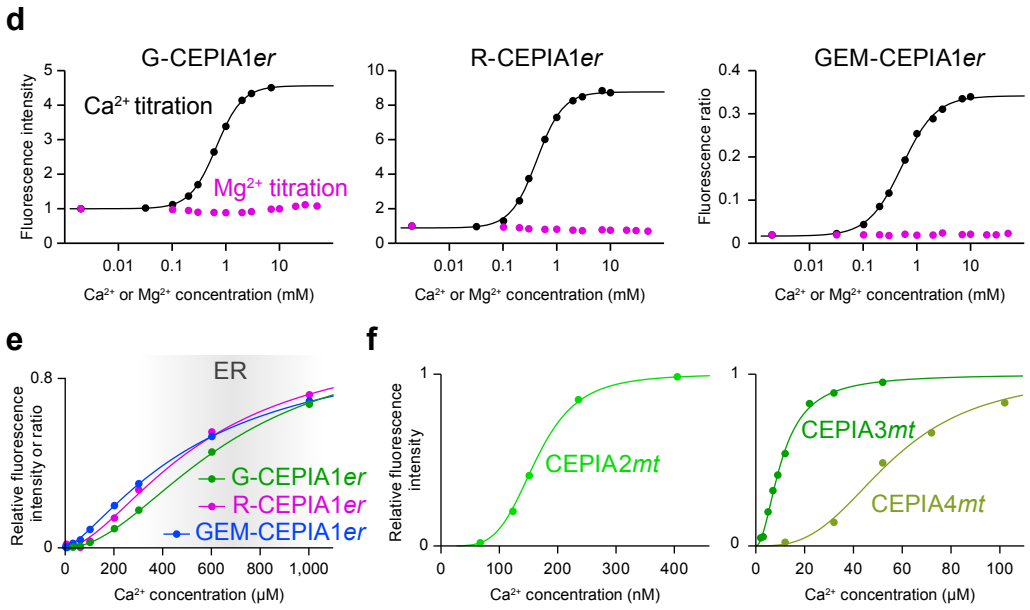

Supplementary Figure 2. *In vitro* properties of CEPIA.

(**a**) Spectral titration curves of CEPIA*er* at various Ca^{2+} concentrations. Fluorescence intensity change was normalized by the maximum intensity. For emission spectra, G-CEPIA1*er*, R-CEPIA1*er* and GEM-CEPIA1*er* were excited at 488, 562 and 395 nm, respectively. For excitation spectra, fluorescence intensity at 512 and 584 nm were obtained for G-CEPIA1*er* and R-CEPIA1*er*, respectively, and at 460 and 510 nm for GEM-CEPIA1*er*.

(**b**) Absorbance spectra of CEPIA*er* (upper panels) and original GECO (lower panels) in Ca^{2+}-containing (5 mM, magenta) or Ca^{2+}-free (1 mM EGTA, black) solution.

(**c**) pH titration curves of CEPIA*er*. The fluorescence intensity or ratio was normalized within the maximum and minimum values. pK_a was evaluated by the pH titration in Ca^{2+}-containing (magenta) or Ca^{2+}-free (black) solution. The plots of G-CEPIA1*er*, G-GECO1.1 and R-GECO1 were fitted by a single Hill plot equation. The plots of R-CEPIA1*er*, GEM-CEPIA1*er*, and GEM-GECO1 were fitted by a double Hill plot equation. All the extracted parameters are summarized in Table 1.

(**d**) Mg^{2+} titration curves of CEPIA*er* (magenta) compared with Ca^{2+} titration curves (black). The fluorescence intensity was normalized within the values in Mg^{2+} and Ca^{2+} free solution.

(**e**) Ca^{2+} titration of G-CEPIA1*er* (green), R-CEPIA1*er* (magenta) and GEM-CEPIA1*er* (blue) plotted against linear $[Ca^{2+}]_{ER}$ scale. Fitted Hill plot curves are also shown. Putative range of Ca^{2+} concentration in the ER is indicated (gray box).

(**f**) Ca^{2+} titration of CEPIA2–4*mt* plotted against linear $[Ca^{2+}]_{ER}$ scale. Fitted Hill plot curves are also shown.

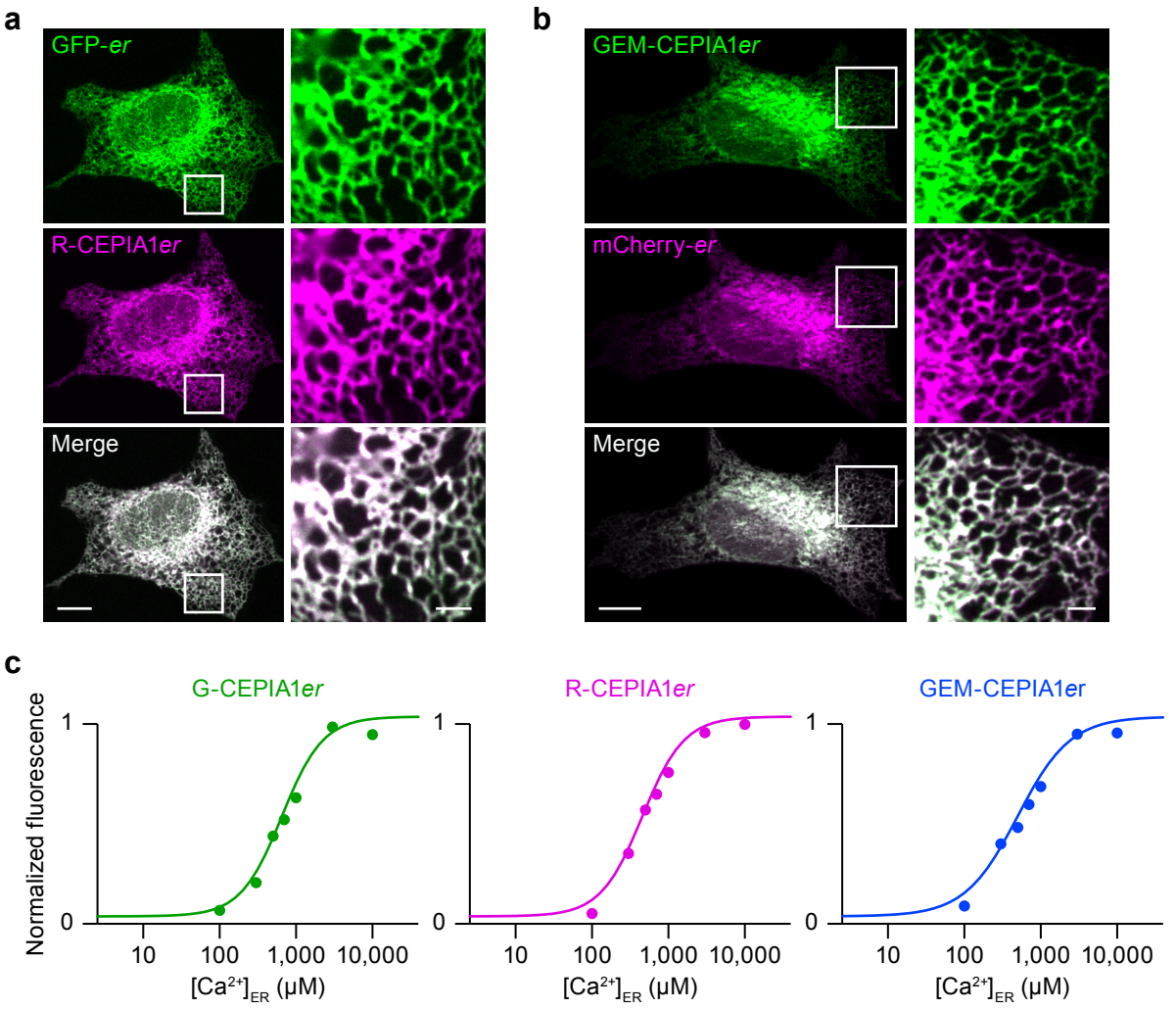

d

Probe	*in situ*			*in vitro*		
	Dynamic range	K_d for Ca^{2+} (μM)	Hill coefficient	Dynamic range	K_d for Ca^{2+} (μM)	Hill coefficient
G-CEPIA1*er*	5.1 ± 0.3	650 ± 17	1.62 ± 0.04	4.7 ± 0.3	672 ± 23	1.95 ± 0.07
R-CEPIA1*er*	4.7 ± 0.2	455 ± 10	1.59 ± 0.04	8.8 ± 0.7	565 ± 58	1.70 ± 0.04
GEM-CEPIA1*er*	10.1 ± 1.6	496 ± 11	1.26 ± 0.02	21.7 ± 0.6	558 ± 14	1.37 ± 0.01

Supplementary Figure 3. Localization and *in situ* Ca^{2+} titration of CEPIA*er*.

(**a** and **b**) Representative images of HeLa cells expressing R-CEPIA1*er* (**a**) or GEM-CEPIA1*er* (**b**). Images were compared with the co-expressed ER-targeted EGFP (**a**) or mCherry (**b**). The images within the white boxes were expanded. Note that the ER signal sequence in CEPIA*er* is different from that of EGFP-er and mCherry-er (See Methods). Scale bars, 10 μm (left) and 2 μm (right).

(**c**) To determine the Ca^{2+} affinity of CEPIA*er* within the ER, HeLa cells expressing one of CEPIA*er* (G-CEPIA1*er*, R-CEPIA1*er* or GEM-CEPIA1*er*) were permeabilized with 150 μM β-escin in a solution containing 3 μM thapsigargin and 3 μM ionomycin. Then Ca^{2+} concentration in the bathing solution was increased in a stepwise manner.

(**d**) Summary of the properties of CEPIA*er* determined by *in situ* Ca^{2+} titration. Note that these parameters were similar to those obtained from *in vitro* Ca^{2+} titration experiments.

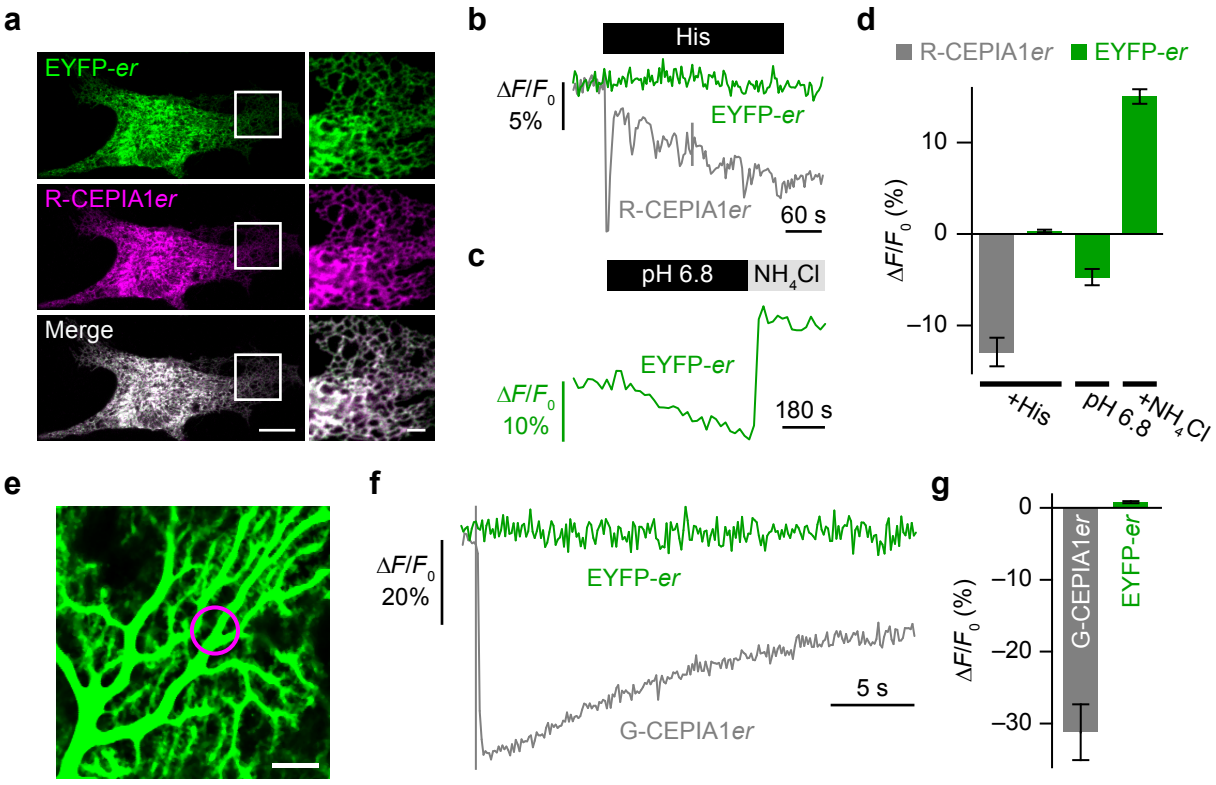

Supplementary Figure 4. CEPIA*er* responses are independent of ER pH dynamics.

(**a**) Confocal images of HeLa cells expressing EYFP-*er* (upper), R-CEPIA1*er* (middle) and the merged image (lower). The images within the white boxes were expanded. Scale bars, 10 μm (left) and 2 μm (right).

(**b**) Simultaneous measurement of EYFP-*er* (green) and R-CEPIA1*er* (gray) in HeLa cells stimulated with 10 μM histamine.

(**c**) pH-dependent changes of EYFP-*er* fluorescence intensity in HeLa cells. The cells were first bathed in an acidic solution (pH 6.8) containing monensin (10 μM) and nigericin (10 μM), and subsequently in an alkalinization solution (30 mM NH_4Cl).

(**d**) Summary of EYFP-*er* and R-CEPIA1*er* responses (mean ± s.e.m., n = 14).

(**e**) Dendrites of EYFP-*er*-expressing Purkinje cells. The magenta circle (10 μm diameter, under the stimulation pipette) indicates the region of interest for panel **f**. Scale bar, 10 μm.

(**f**) The time course of fluorescence intensity change of EYFP-*er* (green) upon PF inputs (10 stimuli at 100 Hz, gray line). For comparison, the fluorescence intensity change of G-CEPIA1*er* displayed in Fig. 3 was shown (gray).

(**g**) Summary of PF-induced responses of G-CEPIA1*er* and EYFP-*er*. Average $\Delta F/F_0$ within the 3-s time window starting from the first PF stimulation pulse (mean ± s.e.m., n = 8).

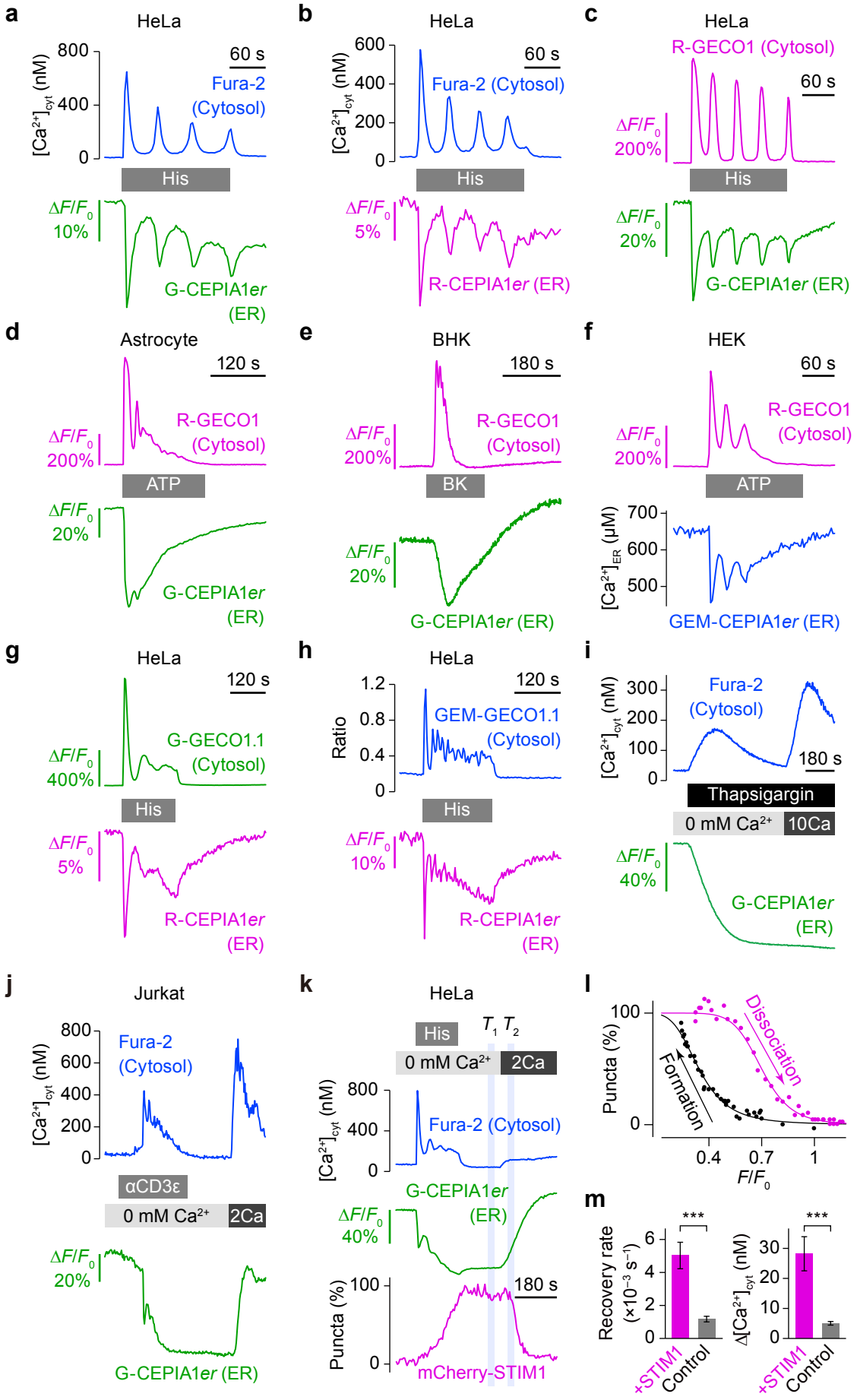
a
HeLa
800
400
0
[Ca2+]cyt (nM)
60 s
Fura-2
(Cytosol)
His
ΔF/F0
10%
G-CEPIA1er
(ER)
b
HeLa
600
400
200
0
[Ca2+]cyt (nM)
60 s
Fura-2 (Cytosol)
His
ΔF/F0
5%
R-CEPIA1er (ER)
c
HeLa
R-GECO1 (Cytosol)
60 s
ΔF/F0
200%
His
ΔF/F0
20%
G-CEPIA1er (ER)
d
Astrocyte
120 s
ΔF/F0
200%
R-GECO1
(Cytosol)
ATP
ΔF/F0
20%
G-CEPIA1er
(ER)
e
BHK
180 s
ΔF/F0
200%
R-GECO1
(Cytosol)
BK
ΔF/F0
20%
G-CEPIA1er (ER)
f
HEK
60 s
ΔF/F0
200%
R-GECO1
(Cytosol)
ATP
700
600
500
[Ca2+]ER (μM)
GEM-CEPIA1er (ER)
g
HeLa
120 s
ΔF/F0
400%
G-GECO1.1
(Cytosol)
His
ΔF/F0
5%
R-CEPIA1er
(ER)
h
HeLa
1.2
0.8
0.4
0
Ratio
120 s
GEM-GECO1.1
(Cytosol)
His
ΔF/F0
10%
R-CEPIA1er
(ER)
i
300
200
100
0
[Ca2+]cyt (nM)
Fura-2
(Cytosol)
180 s
Thapsigargin
0 mM Ca2+
10Ca
ΔF/F0
40%
G-CEPIA1er
(ER)
j
Jurkat
800
600
400
200
0
[Ca2+]cyt (nM)
Fura-2
(Cytosol)
αCD3ε
0 mM Ca2+
2Ca
ΔF/F0
20%
G-CEPIA1er (ER)
k
HeLa
His
T1 T2
0 mM Ca2+
2Ca
800
400
0
[Ca2+]cyt (nM)
Fura-2 (Cytosol)
G-CEPIA1er
(ER)
ΔF/F0
40%
100
0
Puncta (%)
180 s
mCherry-STIM1
l
100
0
Puncta (%)
Dissociation
Formation
0.4
0.7
1
F/F0
m
Recovery rate
(×10−3 s−1)
6
4
2
0
***
+STIM1
Control
Δ[Ca2+]cyt (nM)
30
20
10
0
***
+STIM1
Control

Supplementary Figure 5. Simultaneous measurement of ER Ca^{2+} signals with other fluorescence molecules using CEPIA*er*.

(**a** and **b**) Simultaneous measurement of Ca^{2+} signals in the ER (G-CEPIA1*er* or R-CEPIA1*er*) and cytosol (fura-2) in HeLa cells stimulated with 10 μM histamine.

(**c–f**) Simultaneous Ca^{2+} imaging in the ER (G-CEPIA1*er* or GEM-CEPIA1*er*) and cytosol (R-GECO1) in a HeLa cell (**c**), an astrocyte (**d**), a BHK cell (**e**) or a HEK293A cell (**f**), stimulated with 10 μM histamine (**c**), 30 μM ATP (**d** and **f**) or 100 nM bradykinin (**e**), respectively.

(**g** and **h**) Simultaneous Ca^{2+} imaging in the ER (R-CEPIA1*er*) and cytosol using G-GECO1.1 (**g**) or GEM-GECO1 (**h**) in HeLa cells stimulated with 10 μM histamine.

(**i**) Time courses of cytosolic (upper panel) and ER (lower panel) Ca^{2+} responses to thapsigargin (3 μM) treatment in HeLa cells in the absence of extracellular Ca^{2+}, and to subsequent "Ca^{2+} add back" in the extracellular solution.

(**j**) Time courses of cytosolic (upper panel) and ER (lower panel) Ca^{2+} responses to anti-human CD3ε monoclonal antibody (1 μg/ml, R&D systems) treatment in Jurkat T cells in the absence of extracellular Ca^{2+}, and to subsequent "Ca^{2+} add back" in the extracellular solution.

(**k**) Simultaneous imaging of STIM1 dynamics, ER Ca^{2+} level and cytosolic Ca^{2+} concentration using mCherry-STIM1, G-CEPIA1*er* and fura-2, respectively. Time courses of cytosolic Ca^{2+} concentration (blue), ER Ca^{2+} dynamics (green) and the number of mCherry-STIM1 puncta normalized with the minimum and maximum (magenta). As $[Ca^{2+}]_{ER}$ was depleted with histamine stimulation in the Ca^{2+}-free solution, mCherry-STIM1 formed puncta. After Ca^{2+} addback in the external solution, $[Ca^{2+}]_{ER}$ gradually recovered and mCherry-STIM1 puncta disappeared. We calculated the slope of linear fitting to the G-CEPIA1*er* fluorescence change and the average $[Ca^{2+}]_{cyt}$ change during the time interval between T_1 to T_2 (shown in **m**).

(**l**) The normalized number of mCherry-STIM1 puncta was plotted against normalized G-CEPIA1*er* fluorescence (F/F_0) during puncta formation (black) and dissociation (magenta). The relationship between $[Ca^{2+}]_{ER}$ and puncta formation can be fitted by Hill plot with a Hill coefficient of 8.7 ± 1.1 and a $K_{1/2}$ of 0.37 ± 1.1 for puncta formation, and 6.8 ± 0.6 and 0.60 ± 0.04 for puncta dissociation.

(**m**) Comparison of the ER Ca^{2+} refilling rate and $[Ca^{2+}]_{cyt}$ in response to "Ca^{2+} add back" between STIM1-expressing cells and control cells. Left, the slope of linear fitting to the G-CEPIA1*er* fluorescence change during the time interval between T_1 to T_2 in **k** (middle panel) were shown. Right, the average $[Ca^{2+}]_{cyt}$ change during the time interval between T_1 to T_2 in **k** (upper panel) were show. $n = 35$ for control and 6 for STIM1-expressing cells (mean ± s.e.m.). ***, $P < 0.001$.

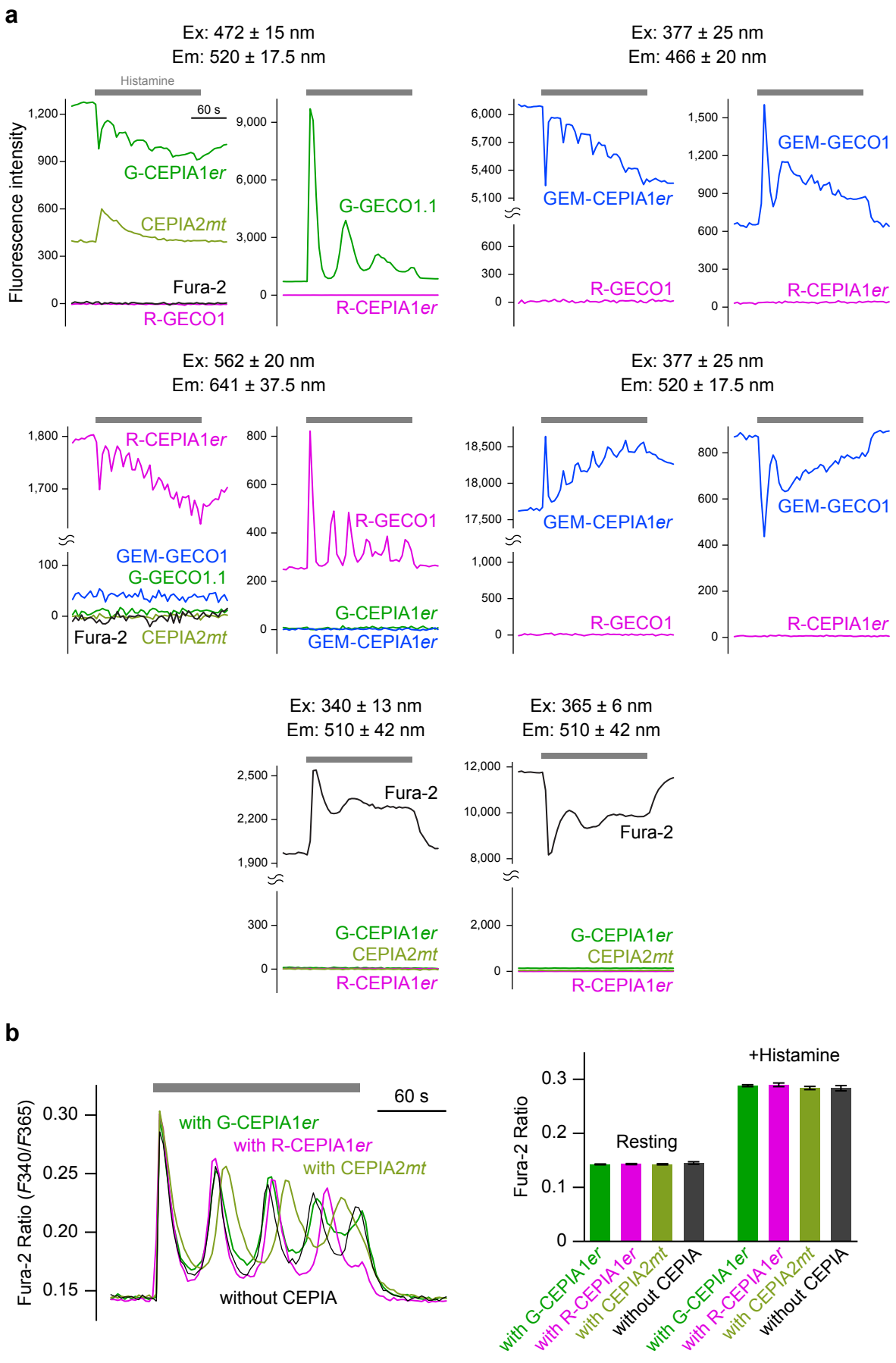
a
Ex: 472 ± 15 nm
Em: 520 ± 17.5 nm
Histamine
60 s
Fluorescence intensity
G-CEPIA1er
CEPIA2mt
Fura-2
R-GECO1
G-GECO1.1
R-CEPIA1er
Ex: 377 ± 25 nm
Em: 466 ± 20 nm
GEM-CEPIA1er
GEM-GECO1
Ex: 562 ± 20 nm
Em: 641 ± 37.5 nm
Ex: 377 ± 25 nm
Em: 520 ± 17.5 nm
Ex: 340 ± 13 nm
Em: 510 ± 42 nm
Ex: 365 ± 6 nm
Em: 510 ± 42 nm
b
Fura-2 Ratio (F340/F365)
with G-CEPIA1er
with R-CEPIA1er
with CEPIA2mt
without CEPIA
Resting
+Histamine
Fura-2 Ratio

Suppementary Figure 6. Bleed-through of CEPIA, GECO and fura-2.

(**a**) Representative traces of fluorescence intensity changes in response to histamine application at six pairs of excitation and emission wavelengths (472/520, 562/641, 377/466, 377/520, 340/510 and 365/510 nm), in HeLa cells expressing one of the genetically encoded indicators or loaded with fura-2. Autofluorescence was subtracted.

(**b**) Comparison of the resting and agonist-induced peak fura-2 ratios among the cells expressing G-CEPIA1*er* (green; $n = 18$, mean ± s.e.m.), R-CEPIA1*er* (magenta; $n = 25$), CEPIA2*mt* (light green; $n = 16$) and cells without CEPIA expression (black; $n = 68$). There were no significant differences in the resting and peak fura-2 ratios. $P = 0.51$ and 0.40, one-way ANOVA.

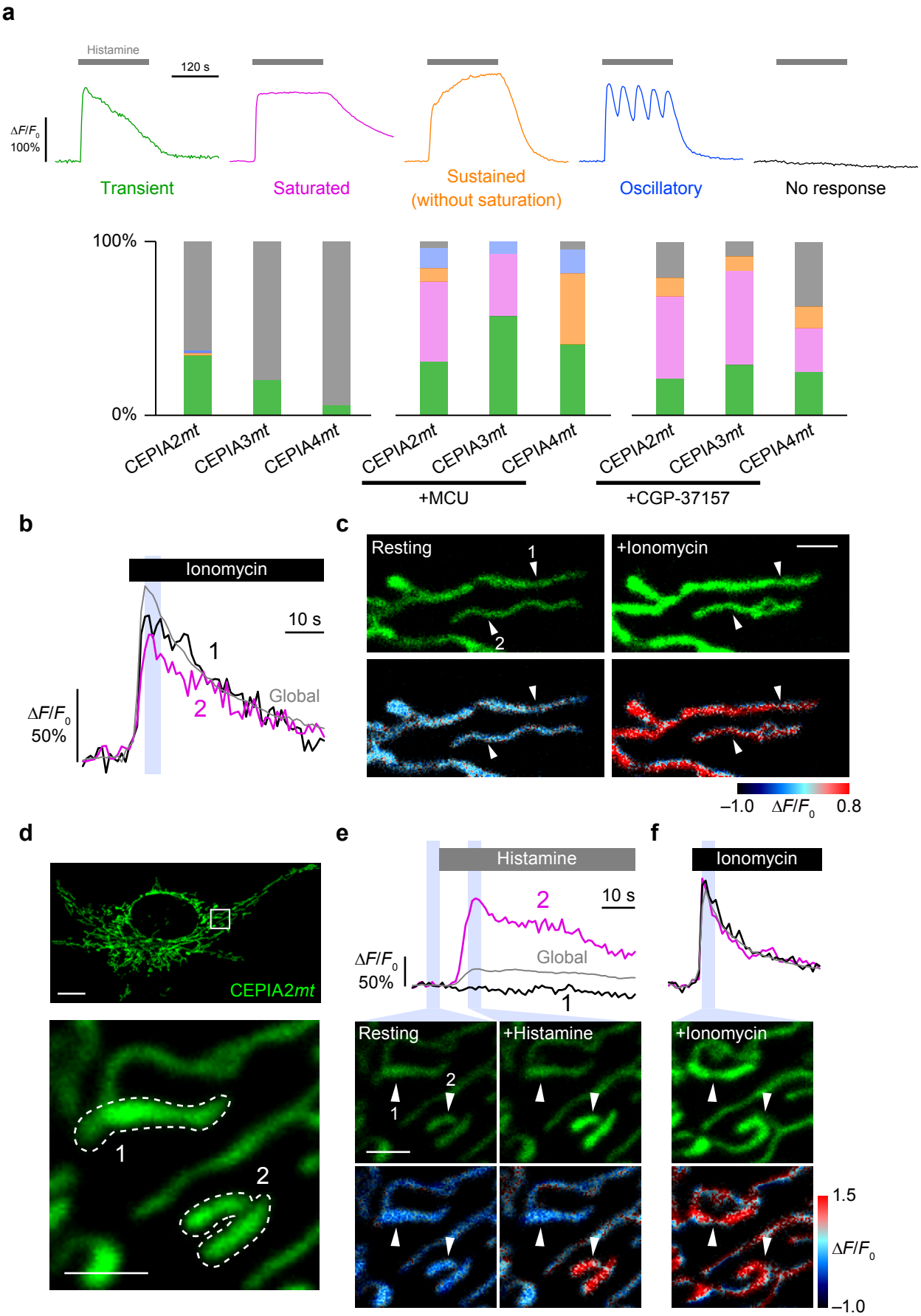
a
Histamine
120 s
ΔF/F0
100%
Transient
Saturated
Sustained
(without saturation)
Oscillatory
No response
100%
0%
CEPIA2mt
CEPIA3mt
CEPIA4mt
+MCU
+CGP-37157
b
Ionomycin
10 s
ΔF/F0
50%
Global
c
Resting
+Ionomycin
–1.0
ΔF/F0
0.8
d
CEPIA2mt
e
Histamine
10 s
ΔF/F0
50%
Global
Resting
+Histamine
f
Ionomycin
+Ionomycin
1.5
ΔF/F0
–1.0

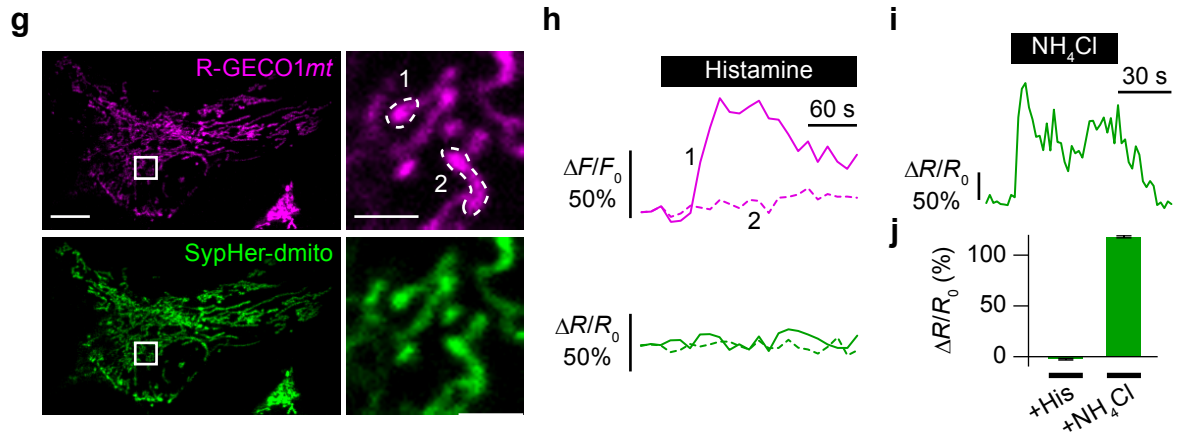

Supplementary Figure 7. Intercellular and subcellular heterogeneity of mitochondrial Ca^{2+} signals.

(**a**) Mitochondrial Ca^{2+} responses measured with CEPIA2–4*mt* during histamine (10 μM) stimulation were compared among control HeLa cells (n = 67, 45 and 35), rat MCU-expressing cells (n = 26, 28 and 22) and CGP-37157 (10 μM)-pretreated cells (n = 19, 24 and 16). The response patterns were classified into five groups: rapid increase followed by slow decay (green), saturated response (magenta), sustained increase without saturation (orange), oscillatory response (blue), and no response (gray).

(**b** and **c**) Subcellular imaging of mitochondrial Ca^{2+} dynamics upon ionomycin application in a HeLa cell expressing CEPIA3*mt*. (**b**) Time courses within the two regions of interest in Fig. 7a and the entire cell (global) were shown. (**c**) Averaged fluorescence images and pseudo-color images at resting state (T_1 in Fig. 7b) and after ionomycin application (blue box) were shown. Scale bar, 2 μm.

(**d**) Fluorescence images of a HeLa cell expressing CEPIA2*mt*. The area within the white box was expanded (lower). Scale bars, 10 μm (upper) and 2 μm (lower).

(**e** and **f**) Time courses within the two regions of interest in **d** and the entire cell (global) were shown upon 10 μM histamine (**e**) and subsequent 3 μM ionomycin (**f**) application. Averaged fluorescence images and pseudo-color images were also indicated. Scale bar, 2 μm.

(**g**) Representative images of HeLa cells expressing R-GECO1*mt* (upper) and a mitochondria-targeted pH indicator SypHer-dmito (lower). The regions within the white boxes were expanded (right). Scale bars, 10 μm (left) and 2 μm (right).

(**h**) Time courses of R-GECO1*mt* (upper) and SypHer-dmito (lower) upon histamine (10 μM) stimulation within the two regions of interest indicated in **g**.

(**i**) pH dependent change of SypHer-dmito fluorescence ratio in the region 1 indicated in **g**. The cells expressing SypHer-dmito were alkalinized with a solution containing 30 mM NH_4Cl.

(**j**) Summary of SypHer-dmito responses. Mitochondria responding with an increase in Ca^{2+} to histamine stimulation were analyzed. The average of $\Delta R/R_0$ after histamine and NH_4Cl stimulation were plotted (n = 89 and 365, respectively; mean ± s.e.m.).

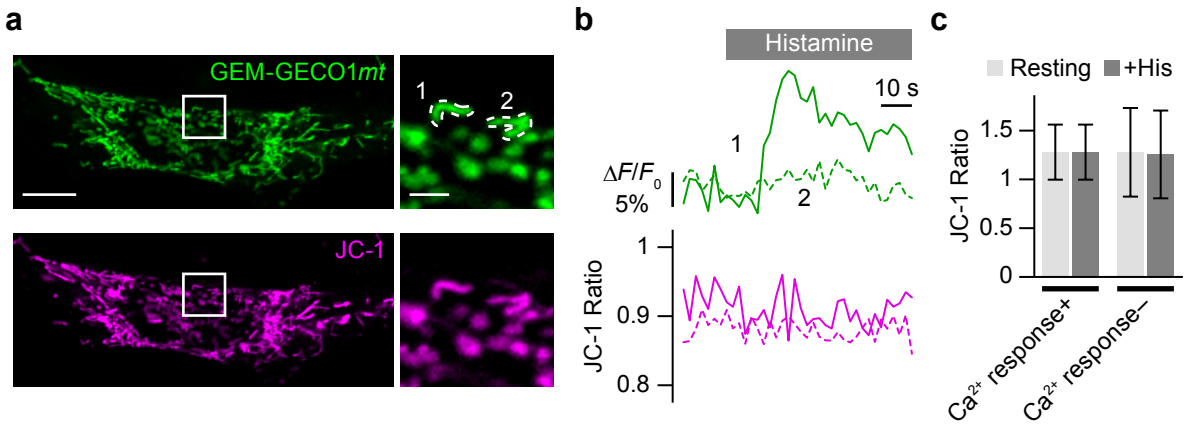

Supplementary Figure 8. Simultaneous imaging of mitochondrial inner membrane potential with heterogeneous Ca^{2+} signal.

(**a**) Representative images of HeLa cells expressing GEM-GECO1*mt* (upper) co-stained with JC-1 (lower). The regions within the white boxes were expanded (right). Scale bars, 10 μm (left) and 2 μm (right).

(**b**) Time courses of GEM-GECO1*mt* (upper) and JC-1 (lower) upon histamine (10 μM) stimulation within the two regions of interest indicated in **a**.

(**c**) Summary of JC-1 ratio in the mitochondria responding with (n = 69, mean ± s.d.) or without (n = 327) an increase in Ca^{2+} concentration to histamine stimulation. The average values within 6-s time window before (gray, Resting) and after (black, +His) histamine application were analyzed.

Supplementary Table 1. CEPIA library.

cfGCaMP2 variants

Mutated amino acids	Dynamic range	Hill coeff.	K_d (μM)
Original (CEPIA2*mt*)	5.1	2.5	0.67
■ Substitutions used in previously reported ER Ca^{2+} indicators			
E11K/E84R/E87K (D1ER)	2.6	0.9	14.5
E31Q (YC4er)	2.5	0.5	64.9
E104Q (YC3er)	3.4	3.7	1.2
■ Single substitution at *–Z* position			
E31D (split-YC7.3er, CEPIA3*mt*)	5.0	1.5	14.5
E67D	4.7	1.4	9.2
E104D	3.8	4.2	0.99
E140D	4.4	3.7	2.1
■ Double substitutions at *–Z* positions			
E31D/E67D	2.6	1.3	470
E31D/E104D	4.1	1.5	20.7
E31D/E140D	4.7	2.0	23.5
E67D/E104D	4.3	1.5	17.9
E67D/E140D	4.7	2.1	23.9
E104D/E140D	4.2	1.2	24.4
■ Triple substitutions at *–Z* positions			
E31D/E104D/E140D	3.2	1.9	135
E67D/E104D/E140D	3.6	2.2	129
■ Substitutions at F92W and/or D133E			
F92W	4.5	3.3	0.90
D133E	4.3	4.7	2.1
F92W/D133E	4.6	3.0	10.3
■ F92W/D133E and single substitutions at *–Z* positions			
E31D/F92W/D133E (CEPIA4*mt*)	4.9	1.7	90.2
E67D/F92W/D133E	4.9	2.3	75.2
F92W/E104D/D133E	3.5	1.3	130
F92W/D133E/E140D	4.5	0.9	67.4
■ F92W/D133E and double substitutions at *–Z* positions			
E31D/F92W/E104D/D133E (CEPIA1*er*)	4.2	1.3	368
E31D/F92W/D133E/E140D	3.5	1.8	411
E67D/F92W/D104D/D133E	4.1	1.9	344
E67D/F92W/D133E/D140D	4.4	1.7	276
F92W/E104D/D133E/E140D*	1.3,2.7	1.9, 1.4	3.7, 1,540
■ D133E and single substitutions at *–Z* positions			
E31D/D133E	5.0	2.2	33.2
E67D/D133E	5.0	2.4	31.1
E104D/D133E	3.5	1.2	43.8
D133E/E140D	4.5	2.2	8.2
■ D133E and double substitutions at *–Z* positions			
E31D/E104D/D133E	4.2	2.0	201
E31D/D133E/E140D	4.7	1.8	92.2
E67D/E104D/D133E	4.1	2.2	154
E67D/D133E/E140D	4.4	1.9	93.4
E104D/D133E/E140D*	1.3, 3.1	1.7, 1.3	4.8, 661
■ Other substitutions			
E11K	2.1	3.6	1.4
E84R/E87K	3.3	2.8	1.2
E31A	1.9	0.8	15.2
E31Q/D133E	2.2	0.6	109
E67D/E104Q	4.2	1.4	43.7
E104Q/E140D	3.1	0.8	23.8
E31Q/F92W/D133E	2.1	0.3	1,730
F92W/E104Q/D133E*	1.5, 1.4	2.0, 0.9	4.3, 6,100
E31D/F92W/E104Q/D133E	1.8	0.6	13,400
E67D/F92W/E104Q/D133E	2.4	0.7	2,330
F92W/S101D/D133E	5.1	3.2	7.0
F92W/D95N/N97D/D133E	4.9	3.2	8.2
F92W/D95N/S101D/D133E	4.3	2.7	11.1
E31D/L36M	4.0	1.1	22.4
E31D/L36M/E67D	2.8	1.2	873
E31D/L36M/E104D	4.0	1.5	25.0
E31D/L36M/E140D	4.9	2.0	26.1
E31D/L36M/E104Q	3.8	1.5	45.2
T26G/E31D/L36M	4.6	0.9	2.4
E31D/L36M/Q41L	3.9	1.3	15.1
E31D/L36M/K75I	3.7	1.2	9.2
E31D/L36M/Q41L/K75I	3.1	1.1	8.9

R-GECO1 variants with cfGCaMP2 CaM

Mutated amino acids	Dynamic range	Hill coeff.	K_d (μM)
E31D/E67D	17.6	1.2	152
E31D/F92W/D133E	21.9	2.3	16.6
E31D/E104D/D133E	19.8	2.7	26.3
E104D/D133E/E140D	12.5	1.4	50.8
E31D/E67D/F92W/D133E	17.2	1.2	211
E31D/F92W/E104D/D133E	16.9	2.3	70.9
E67D/F92W/D133E/E140D	17.6	2.1	20.0
F92W/E104D/D133E/E140D	14.9	1.0	123
E31D/E67D/F92W/E104D/D133E (R-CEPIA1*er*)	8.8	1.7	565

G-GECO1.1 variants with cfGCaMP2 CaM

Mutated amino acids	Dynamic range	Hill coeff.	K_d (μM)
E31D/F92W/D133E	10.2	1.5	209
E31D/F92W/E104D/D133E (G-CEPIA1*er*)	4.7	1.9	672
E31D/E67D/F92W/E104D/D133E	3.8	0.5	3,860

GEM-GECO1 variants with cfGCaMP2 CaM

Mutated amino acids	Dynamic range	Hill coeff.	K_d (μM)
E31D/F92W/E104D/D133E	1.1	n.d.	n.d.
E31D/E67D/F92W/E104D/D133E	1.2	n.d.	n.d.

GEM-GECO1 variants with original CaM

Mutated amino acids	Dynamic range	Hill coeff.	K_d (μM)
Original	67.5	2.6	0.31
E31D	23.7	1.2	7.2
E31D/E67D	13.0	1.2	97.1
E31D/D133E	41.3	2.4	36.4
E31D/E140D	43.6	2.2	24.2
E31D/F92W/D133E	11.2	1.9	90.0
E31D/E104D/D133E	20.8	1.7	89.7
E31D/D133E/E140D	24.8	1.6	147
E31D/F92W/E104D/D133E	8.1	2.1	225
E31D/F92W/D133E/E140D (GEM-CEPIA1*er*)	21.7	1.4	558
E31D/E104D/D133E/E140D	34.8	1.5	483
E31D/E67D/F92W/D133E/E140D	1.4	1.1	602
E31D/F92W/E104D/D133E/E140D	2.3	1.0	2,010

CEPIA library generated in the present study. The properties of CEPIA variants that were used in the intraorganellar Ca^{2+} imaging are highlighted (magenta). cDNAs were confirmed by sequencing.

*Ca^{2+} titration curves were obtained by fitting with a double Hill plot equation.

Supplementary Table 2. The list of primers and oligonucleotides.

Primer number		Sequence
1		ATAAGCATATGCAGGTCCAACTGCAGGGAT
2		ATTAGATCTCTACAGCTCGTCCTTCTCGCT
3		AGAGGATCCATGGTCGACTCTTCACGTCGT
4		TAGCGGCCGCCTTCGCTGTCATCATTTGTA
5		GAGACCAACTGACTGAAGAGCAGATCGCAG
6		GAGTAGCCTCCCAGCCCATGGTCTTCTTCT
7		GCAACACTCGAGACCAACTGACTGAAGAGC
8	(E11K)	GCTGACTGAAGAGCAGATCGCAAAATTTAA
9	(E11K)	TGGTCACGCGTGTTGTACTCCAGCTT
10	(E31D)	GGGCAGAACCCCACAGAAGCAGAGCTCCAG
11	(E31D)	CAGAGACCGCAGCACCGTCCCCAGATCCTT
12	(E31D)	CAGAGACCGCATCACCGTCCCCAGATCCTT
13	(E31Q)	CTGGGGACGGTGCTGCGGTCTCT
14	(E31Q)	CTGCTTGGTTGTTATTGTCCCATCCCCGTC
15	(E67D)	GACAATGATGGCAAGAAAAATGAAAGACAC
16	(E67D)	GACGATGATGGCAAGAAAAATGAATGACAC
17	(E67D)	GACAATGATGGCACCTAAAATGCAGGACAC
18	(E67D)	AGGAAATCAGGGAAGTCGATTGTGCCATTA
19	(E67D)	AGGAAATCAGGGAAGTCGAAGGTACCGTCA
20	(E67D)	AGGAAATCAGGGAAGTCGATGGTACCGTCA
21	(E84R/E87K)	AATTCGAAAAGCGTTCCGTGTGTTTGATAA
22	(E84R/E87K)	CTTTCTTCACTGTCTGTGTCTTTCATTTTT
23	(F92W)	GGGATAAGGATGGCAATGGCTACATCAGT
24	(F92W)	ACACACGGAACGCTTCGCGAATTTCTTCT
25	(F92W)	GGGATAAGGATGGCAATGGCTACATCGGC
26	(E104D)	AGCAGACCTTCGCCACGTGATGACAAACCT
27	(E104D)	AGCAGATCTTCGCCACGTGATGACAAACCT
28	(E104D)	AGCAGATCTTCGCCACGTGATGACAGACCT
29	(E104D)	GCGCCGATGTAGCCATTGCCGTCCTTATC
30	(E104Q)	GCAGAGATGTAGCCATTGCCATCCTTATC
31	(E104Q)	AGCACAGCTTCGCCACGTGATGACAAACCT
32	(D133E)	ATCGATGGAGAAGGTCAGGTAAACTACGAA
33	(D133E)	ATCTGCTTCCCTGATCATTTCATCAACCTC
34	(D133E)	GTCTGCTACCCTGATCATTTCATCAACCTC
35	(E140D)	ATGATGACAGCGAAGGCGGCCGCAGAACAA
36	(E140D)	TTGTACAAAGTCTTCGTAGTTTACCTGACC
37		AGGGATCCATGCGGGGTTCTCATCATCATC
38		GGGATCCATCATCATCATCG
39		TCGACGATGATGATGATGGATCCCTGCA
40		CGCGCCAAAATTCATTCACTGGGGGACCCC
41		ATGAGCGTGCTCACCCCACTCCTGCTGCGGGGGCTGACCG
42		GCAGCGCTAGGCGGCTGCCAGTCCCGCGG
43		GCCAAGATCCACAGTCTCGGCGATCCCG
44		TCATGGGGTCCCCCAGTGAATGAATTTTGG
45		CTGCCGGTCAGCCCCCGCAGCAGGAGTGGGGTGAGCACGC
46		TGGCCCGCGGGACTGGCAGCCGCCTAGCG
47		GATCCGGGATCGCCGAGACTGTGGATCT
48		ATAAGCTTGCCACCATGGGATGGAGCTGTA
49		AGAACTAGTCTACAGCTCGTCCTTCTCGCT
50		GATCCATGCTGCTGCCCGTCCCCCTGCTGC
51		TGGGCCTGCTGGGCGCCGCCGCCGACATGG
52		CCCAGCAGCAGGGGGACGGGCAGCAGCATG
53		TCGACCATGTCGGCGGCGGCGCCCAGCAGG
54		AAACCGCGGACATGGTGAGCAAGGGCGAGG
55		GACGAATTCTTACAGCTCGTCCTTCTTGTACAGCTCGTCCATGC
56		AAGCCGCGGACATGGTGAGCAAGGGCGAGG
57		GCCGAATTCTTACAGCTCGTCCTTCTTGTACAGCTCGTCCATGC
58		CCGGGCGAATTCGGCAGATATCCATCACAC
59		GATGATGATGGGATCCTCTCATGTCCGCGG
60		CTCGGATCCATGGTGAGCAAGGGCGAGGAG
61		TTAATGCGGCCGCGCCGAGAGTGATCCCGG
62		TGTCTGCAGGCTACAACAGCGACAACGTCT
63		TTGCCTGATCGCGCAAAGAGTGACCATCTT
64		ATATCTAGAGCCACCATGGATGTGTGCGCC
65		CGCCTCTAGACTACTTCTTAAGAGGCTTCT
66		CTTGTACAGCTCGTCCATGCCGCCGGTGGA

The primers and oligonucleotides used in the present study were listed. For the primers used for site-directed mutagenesis, the target mutation sites are indicated in parentheses.